cells

MDPI

Article

Wnt Signaling Rescues Amyloid Beta-Induced Gut Stem Cell Loss

Prameet Kaur [1], Ellora Hui Zhen Chua [1], Wen Kin Lim [1], Jiarui Liu [1], Nathan Harmston [1,2] and Nicholas S. Tolwinski [1,*]

[1] Division of Science, Yale-NUS College, Singapore 138527, Singapore; prameet.k87@gmail.com (P.K.); ellora.chua@yale-nus.edu.sg (E.H.Z.C.); wenkinlim@gmail.com (W.K.L.); jiarui_liu@u.yale-nus.edu.sg (J.L.); nathan.harmston@yale-nus.edu.sg (N.H.)

[2] Program in Cancer and Stem Cell Biology, Duke-NUS Medical School, Singapore 169857, Singapore

* Correspondence: nicholas.tolwinski@yale-nus.edu.sg; Tel.: +65-66013092

Abstract: Patients with Alzheimer's disease suffer from a decrease in brain mass and a prevalence of amyloid-β plaques. These plaques are thought to play a role in disease progression, but their exact role is not entirely established. We developed an optogenetic model to induce amyloid-β intracellular oligomerization to model distinct disease etiologies. Here, we examine the effect of Wnt signaling on amyloid in an optogenetic, *Drosophila* gut stem cell model. We observe that Wnt activation rescues the detrimental effects of amyloid expression and oligomerization. We analyze the gene expression changes downstream of Wnt that contribute to this rescue and find changes in aging related genes, protein misfolding, metabolism, and inflammation. We propose that Wnt expression reduces inflammation through repression of Toll activating factors. We confirm that chronic Toll activation reduces lifespan, but a decrease in the upstream activator Persephone extends it. We propose that the protective effect observed for lithium treatment functions, at least in part, through Wnt activation and the inhibition of inflammation.

Keywords: Alzheimer's disease; amyloid-β; Wnt; *Drosophila*

Citation: Kaur, P.; Chua, E.H.Z.; Lim, W.K.; Liu, J.; Harmston, N.; Tolwinski, N.S. Wnt Signaling Rescues Amyloid Beta-Induced Gut Stem Cell Loss. *Cells* **2022**, *11*, 281. https://doi.org/10.3390/cells11020281

Academic Editors: Stephen Yarwood and Kermit L. Carraway

Received: 28 October 2021
Accepted: 13 January 2022
Published: 14 January 2022

1. Introduction

Alzheimer's disease (AD) is an age-related disease affecting millions of people worldwide [1,2]. No effective therapy exists, despite some recent clinical trials and one controversial new drug which has been recently approved [3–5]. AD drug development has primarily been based on the amyloid cascade hypothesis, with many drugs targeting amyloid beta (Aβ) directly [6,7]. The hypothesis postulates that the extracellular deposition of Aβ leads to neuronal cell death driving AD [8], but whether these plaques are causative remains controversial, due to observations of plaques in asymptomatic individuals [9].

Aβ extracellular aggregates form macroscopic plaques that correlate with cell loss, but Aβ can also form smaller oligomers with soluble oligomers showing the highest toxicity [10]. We recently described an optogenetic method to study Aβ protein oligomerization in vivo in several model organisms [11]. Optogenetics refers to genes that are modified with a light responsive protein domain, allowing the spatial and temporal regulation of proteins [12]. Temporal and spatial control is achieved by light exposure of a specific wavelength, without the need to introduce other external agents [13,14]. We used a modified version of the *Arabidopsis thaliana* cryptochrome 2 (CRY2) protein, which clusters in response to blue light [15].

The Wnt signaling pathway defines several developmental processes in a variety of organisms through two or more branches [16,17]. The canonical pathway defines cell fates, and the non-canonical pathway is involved in cell polarity; for example, in *Drosophila* intestinal stem cells, two Wnt pathway branches are required for stem cell maintenance and regeneration [18–21]. In adults, Wnts play a role in a variety of diseases in addition

to cancer [16,22,23]. Alzheimer's disease and Wnt were linked [24], where Wnt regulates a number of stem cell processes, lipid, glucose, and brain signaling pathways [17,25–27] through a complex signaling cascade [28–30]. In AD, GSK3 and TCF, the regulatory kinase and the main Wnt transcription factor respectively, were linked with disease risk [31,32]. These findings suggested that Wnt modulation could affect the disease state [33,34].

Our previous studies focused on neurogenesis and metabolism, as well as interventions that could ameliorate the condition [11,35]. We showed that lithium worked well to extend the lifespan of *C. elegans* and *Drosophila* in optogenetic Aβ models. We posited that the Wnt signaling pathway may be involved but did not delineate the pathway through which lithium worked. Here, we present evidence that Wnt signaling can ameliorate the detrimental effects of Aβ oligomerization by promoting stem cell homeostasis and preventing inflammation. We speculate that Wnt activators could function in various tissues affected by amyloid or amyloidosis.

2. Materials and Methods

2.1. Crosses and Expression of UAS Construct

Optogenetic transgenes were generated as previously described in [11,36]. Expression was driven by Elav-GAL4, the neuronal driver, *Escargot*-GAL4 [37], and tubP-GAL80^{ts} [38]. All additional stocks were obtained from the Bloomington *Drosophila* Stock Center (NIH P40OD018537) that were used in this study.

Fly lines:

Elav-Gal4: BDSC 458 [39]
Repo-QF2: BDSC 66477 [40]
QUAS-6XGFP: BDSC 52263 [41]
UAS-Aβ-CRY2-mCherry: [11]
UAS-mCD8.RFP: BDSC 32220 [42]
UAS-wg: BDSC 5918 [43]
UAS-Td-Tomato: BDSC 36328 (Joost Schulte and Katharine Sepp)
Tl(CRISPaint.T2A-GAL4)wg: BDSC #83627 [44]
UAS-10XGFP: BDSC 32185 [42]
Esg-Gal4, UAS-GFP; tub-Gal80^{ts}, UAS-dCas9.VPR: BDSC 67069 [45]
UAS-myr::tdTomato: BDSC 32222 [42]
UAS-Toll-Cry2-mCherry: [46]
Arm-Gal4: BDSC 1560 [47]
ArmGal4; tub-GAL80^{ts}: BDSC 86327 [38]
TRiP.HMC03615 attP40 Persephone RNAi [48]
TRiP.HM05191 attP2 Dif RNAi [48]
UAS-Dsh [49].

Fly crosses performed were:

(1) Elav-Gal4; Repo-QF2, QUAS-GFP × UAS-Aβ-CRY2-mCh
(2) Elav-Gal4, UAS-RFP × UAS-wg
(3) Elav-Gal4 × UAS-Td-Tomato
(4) Tl(CRISPaint.T2A-GAL4)wg × UAS-10XGFP
(5) w; UAS-TdTomato X esg-Gal4, UAS-GFP; tubP-GAL80^{ts}
(6) w; UAS-Aβ^{1-42}-CRY2-mCh X esg-Gal4, UAS-GFP; tubP-GAL80^{ts}
(7) w; UAS-wg; UAS-Aβ^{1-42}-CRY2-mCh X esg-Gal4, UAS-GFP; tub-GAL80^{ts}
(8) w; UAS-wg, UAS-myr-Tomato × esg-Gal4, UAS-GFP; tub-GAL80^{ts}
(9) w; UAS-wg × esg-Gal4, UAS-GFP; tub-GAL80^{ts}
(10) w; UAS-Toll-Cry2-mCh × esg-Gal4, UAS-GFP; tub-GAL80^{ts}
(11) w; UAS-Toll-Cry2-mCh × ArmGal4; tub-GAL80^{ts}
(12) w; UAS-Td-Tomato × esg-Gal4, UAS-GFP; tub-GAL80^{ts}
(13) w; UAS-Td-Tomato × ArmGal4; tub-GAL80^{ts}
(14) w; UAS-Persephone-RNAi × ArmGal4; tub-GAL80^{ts}

(15) w; UAS-Dif-RNAi × ArmGal4; tub-GAL80^{ts}.

2.2. Light-Sheet Microscopy

Embryos at stage 11 were selected using halocarbon oil (Sigma), dechorionated and mounted into the Lightsheet Z.1 (Carl Zeiss, Oberkochen, Germany) microscope, and imaged with a 40× W Plan-Apochromat 40× 1.0 UV–VIS detection objective [30,50,51]. Image data were processed using the maximum intensity projection function of ZEN 2014 SP software (Carl Zeiss, Oberkochen, Germany).

2.2.1. Gut Preparations and Fluorescence Microscopy

Adult fly midguts from at least 3 flies were dissected and imaged at the 25th percentile from the anterior midgut on the Zeiss LSM800 (Carl Zeiss, Oberkochen, Germany), as described by Bunnag et al. 2020. Images were processed using the ZEN 2014 SP1 software (Carl Zeiss, Oberkochen, Germany). Image quantification was done in ImageJ (Developed by the National Institutes of Health, Bethesda, MD, USA [52]).

2.2.2. RNA Preparation and RNA-Sequencing

Flies were dissected in 1 × PBS. RNA was isolated from at least 10 midguts using the Isolate II RNA Mini kit (Bioline, London, UK). The extracted RNA was quantified using Nanodrop (Thermo Fisher Scientific Waltham, Massachusetts, MA, USA). Library preparation was performed using 1 µg of total RNA, and sequencing was performed using an Illumina HiSeq 4000 System (2 × 151 bp read length, 40 million reads per sample) by NovogeneAIT Genomics (Singapore).

2.2.3. RNA-Seq Analysis

Data processing and QC: RNA-seq was aligned against BDGP6.22 (Ensembl version 97) using STAR v2.7.1a [53], and quantified using RSEM v1.3.1 [54]. Reads mapping to genes annotated as rRNA, snoRNA, or snRNA were removed. Genes which had less than 10 reads mapping on average across all samples were also removed. A differential expression analysis was performed using DESeq2 [55]. The likelihood ratio test (LRT) was used to identify any genes that show change in expression across the different conditions. Pairwise comparisons were performed using a Wald test, with independent filtering. To control for false positives due to multiple comparisons in the genome-wide differential expression analysis, the false discovery rate (FDR) was computed using the Benjamini–Hochberg procedure. The gene level counts were transformed using a regularized log transformation, converted to z-scores, and clustered using partitioning around medoids (PAM), using correlation distance as the distance metric.

Functional enrichment analysis: Gene ontology (GO) and KEGG pathway enrichments for each cluster were performed using EnrichR [56–58]. Terms with an FDR < 10% were defined as significantly enriched.

2.2.4. Lifespan Studies

Drosophila were counted daily for the number of dead subjects and the number of censored subjects (excluded from the study). *Drosophila* that failed to respond to taps were scored as dead, and those stuck to the food were censored. Lifespan analysis was performed using OASIS 2 (Online Application for Survival Analysis 2) [59]. Raw numbers are available for images in Supplementary Tables S4–S6.

3. Results

To study the role of intracellular Aβ, we developed a system of expression coupled with light inducible oligomerization (Figure 1a). Previously, we showed a distinction between the simple overexpression of Aβ and light-induced aggregation, where one led to metabolic changes [35], and the second led to the physical damage of the nervous system [11]. In *Drosophila*, transgenic animals expressed the 42-amino-acid human Aβ

peptide fused to Cryptochrome 2 and the fluorescent protein mCherry ($A\beta^{1-42}$-CRY2-mCh, Figure 1a). Expression in *Drosophila* used the GAL4/UAS system [37] with Elav-Gal4 driving expression in neurons (Videos S1 and S2, Figure 1). Glial cells were imaged using the QUAS system with repo-QF2 driving QUAS-GFP [40]. We imaged embryonic neurogenesis in detail, and observed the physical breakdown of the central nervous system upon Aβ oligomerization (Videos S1 and S2, Figure 1b,c). In lifespan analysis, we observed a rescue of Aβ-induced lifespan shortening through treatment with lithium but were unable to introduce lithium into embryos to test its effect on neurogenesis [11]. We proposed that the rescue may be due to Wnt signaling and attempted to test this in our embryonic system by expressing Wingless (Wg or Wnt1) in developing embryos. However, the expression of Wg in the developing nervous system was not successful, as embryos ceased to develop (Videos S3 and S4, Figure 1d,e). In order to establish the effect of Wnt signaling on Aβ-activity, we moved to an adult system where Wnt is involved in tissue homeostasis through its ability to maintain stem cells, the *Drosophila* gut.

The *Drosophila* gut has rapidly been established as a simple, accessible model for homeostasis, regeneration, and proliferation [60]. The tissue is composed of four cell types: enterocytes (ECs or absorptive cells), enteroendocrine (EEs or secretory cells), enteroblasts (EBs or transit amplifying cells) and intestinal stem cells (ISCs). ISCs rest on the external surface of the gut epithelium away from the gut lumen, and divide symmetrically to generate more ISCs, or asymmetrically to form EBs (Figure 2a) [61]. We confirmed the presence of gut Wg expression by imaging the midgut where a wg-Gal4 enhancer drove the expression of GFP (Figure 2b). As previously shown, expression was most prevalent in the compartment boundaries and stem cell niches [20,21]. In normal guts, ISCs are sparse, and are specifically marked by the expression of *escargot*. Therefore *esg* can be used to drive exogenous GAL4 and activate UAS-GFP or another UAS driven gene specifically in ISCs [45]. We expressed $A\beta^{1-42}$-CRY2-mCh in this tissue and imaged the effect on ISCs. In flies kept in the dark where optogenetic oligomerization was inactive, there was a dramatic increase in GFP-positive cells, especially in transit amplifying, EBs (Figure 3a–a", wildtype guts show an average of five ISCs and no EBs per imaged segment, whereas $A\beta^{1-42}$-CRY2-mCh (Figure 3b–b") expressing guts show ~9 ISCs and ~24 EBs per imaged segment). This effect was completely abrogated by the co-expression of Wg along with $A\beta^{1-42}$-CRY2-mCh, where we observed an increase in total ISCs, but no increase in EBs (Figure 3c–c", $A\beta^{1-42}$-CRY2-mCh + Wg expressing guts showed ~14 ISCs and ~2 EBs). We compared the effect on flies kept in the dark (no optogenetic oligomerization) to flies exposed to light (blue light-induced CRY2-based oligomerization). We observed a small increase in GFP-positive EBs (Figure 3d–d", $A\beta^{1-42}$-CRY2-mCh + Light expressing guts showed on average 5 ISCs and 34 EBs) and a clear loss of EBs, as well as an increase in the number of ISCs following co-expression of Wg along with $A\beta^{1-42}$-CRY2-mCh (Figure 3e–e", $A\beta^{1-42}$-CRY2-mCh + Wg + Light expressing guts showed on average 22 ISCs and 2 EBs). The expression of Wg alone led to an increase in ISC numbers (Figure 3f–f", Wg expressing guts showed on average 15 ISCs and 2 EBs). Together, these findings suggest that either the overexpression or light-induced oligomerization of $A\beta^{1-42}$-CRY2-mCh led to asymmetric stem cell divisions and dramatically altered tissue homeostasis. However, most importantly, tissue homeostasis was restored following the overexpression of Wg.

The expression of $A\beta^{1-42}$-CRY2-mCh in whole organisms, or specifically in the nervous system, led to decreased life and health spans in a light-dependent manner [11]. We postulated that the loss of homeostasis observed in the *Drosophila* gut would be detrimental to adult survival, and so tested the lifespans of flies expressing amyloid and Wg in ISCs. We observed a significant decrease in the survival of flies expressing $A\beta^{1-42}$-CRY2-mCh grown in the light (Figure 4). This effect was rescued by the expression of Wg alongside. Wg expression alone was detrimental as well, but the effect was equivalent to $A\beta^{1-42}$-CRY2-mCh combined with Wg, suggesting that Wg rescued the $A\beta^{1-42}$-CRY2-mCh effects, but still led to other detriments. Please note the increase in ISCs observed in Wg overexpressing guts

suggesting ISC proliferation, perhaps leading to stem cell exhaustion, which may explain the reduction in lifespan for flies overexpressing Wg (Figure 3).

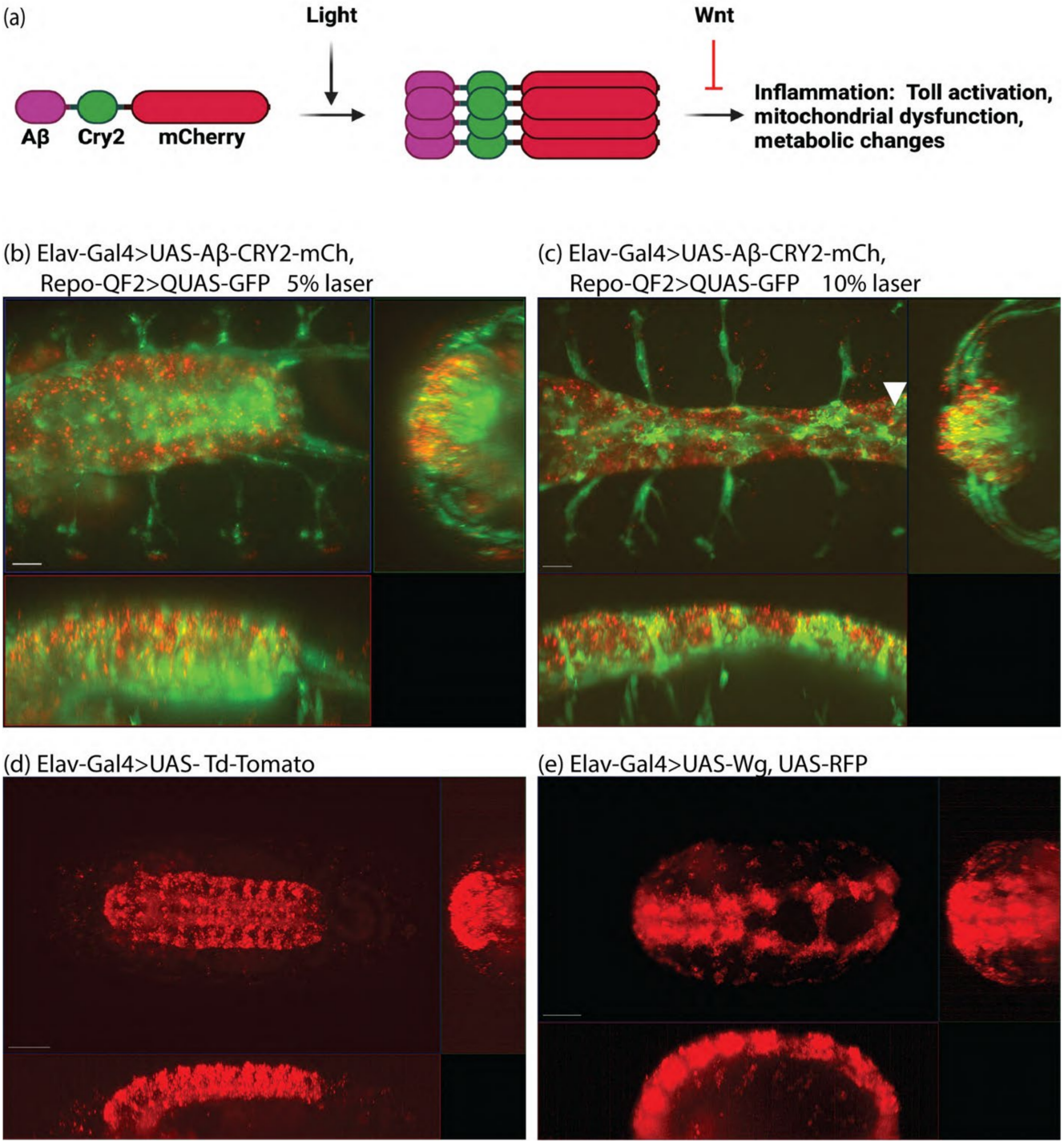

Figure 1. The optogenetic amyloid system in embryos. (**a**) Scheme of light-induced Aβ-Cry2mCh clustering in *Drosophila melanogaster* resulting in activation of inflammatory processes which can be rescued by Wnt. Stills from Video S1 (**b**), Video S2 (**c**), Video S3 (**d**), Video S4 (**e**). Arrowhead is pointing to nervous system constriction.

The finding that Wg rescued both the homeostatic and lifespan deficits caused by Aβ expression in ISCs strongly supports our hypothesis that the inhibition of glycogen synthase kinase 3 (GSK-3) by lithium, leading to the subsequent activation of the Wnt pathway, was

responsible for the observed differences in survival (Figure 4c) [11]. To identify the potential pathways and mechanisms responsible for this rescue, we collected *Drosophila* guts from flies exposed to light, expressing Aβ^{1-42}-CRY2-mCh (Aβ), Wg alone (Wg), Aβ^{1-42}-CRY2-mCh and Wg together (WgAβ), or control flies (WT) expressing only a fluorescent protein, and performed RNA-seq (Figure 5a). Our analysis identified 2800 genes (FDR < 10%) as significantly differentially expressed across the conditions (Figure 5b, Supplemental Table S1). The clustering of these genes identified six distinct clusters, each representing groups of genes with similar expression profiles across the four conditions investigated (Figure 5b,c).

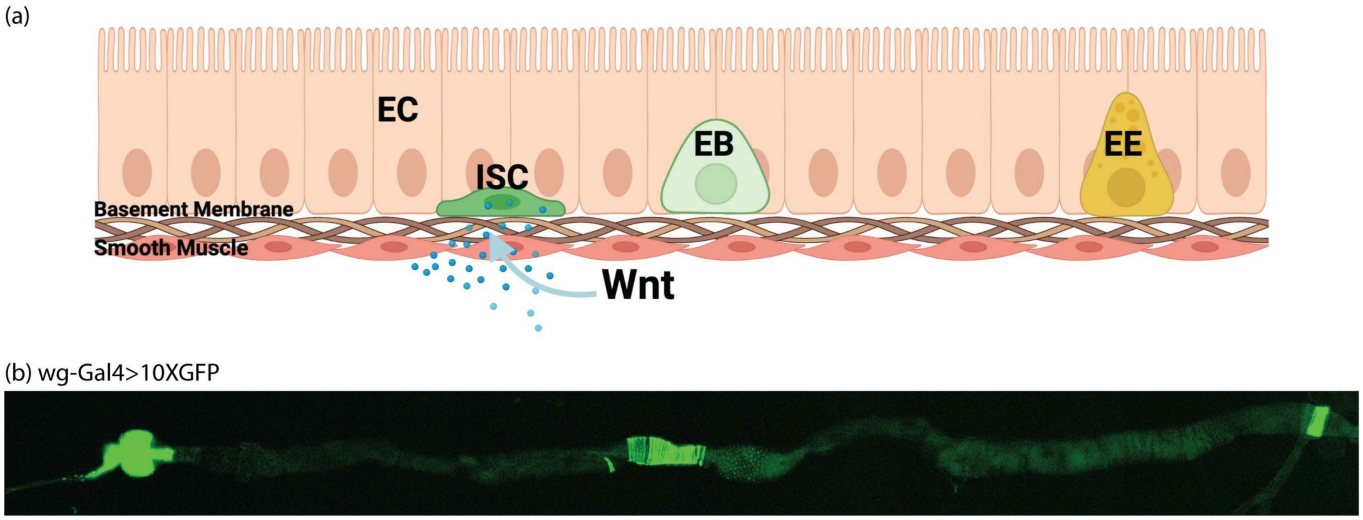

Figure 2. Wnt expression in the *Drosophila* gut. (**a**) Model of the *Drosophila* gut comprising enterocytes (ECs), enteroendocrine (EEs), enteroblasts (EBs) and intestinal stem cells (ISCs). ISCs rest on the external surface of the gut epithelium away from the gut lumen and divide symmetrically to make more ISCs or asymmetrically to form EBs. (**b**) Representative midgut section of a wg-Gal4 > 10× GFP fly.

Each of the six clusters was enriched for distinct pathways and processes (Figure 5d,e, Supplemental Tables S2 and S3). Cluster I (N = 440) contained genes that were upregulated by expression of Aβ^{1-42}-CRY2-mCh, but were repressed by increased Wnt signaling. Genes in this cluster were associated with peroxisome, transport, and metabolic processes (Supplemental Figure S1). Multiple studies have previously directly implicated the peroxisome in mediating AD pathology [62], and have implicated metabolic changes in the disease [63]. Conversely, the genes in Cluster II (N = 273) consisted of genes repressed by Aβ^{1-42}-CRY2-mCh, but whose expression was rescued following the activation of Wnt signaling. This cluster was enriched for processes associated with autophagy, lysosomal activity (Supplemental Figure S2), and the regulation of signaling pathways whose activation has previously been found to be protective against AD, e.g., EGFR, FoxO, and mTOR [23,64,65]. Cluster III (N = 785) and Cluster IV (N = 630) consisted of genes that were Wnt-repressed or Wnt-activated respectively, i.e., were up- or down-regulated following the overexpression of Wg, but the expression of Aβ^{1-42}-CRY2-mCh had no effect on their expression. Cluster III was enriched for ribosome and translation-related processes, whereas Cluster IV was enriched for the Wnt signaling pathway and contained known Wnt target genes (e.g., *Notum*). Cluster V (N = 285) represented genes that were downregulated in the WT condition but were upregulated in all other conditions, while the genes in Cluster VI (N = 387) displayed the opposite pattern. It is likely that these two clusters simply represent the effects of perturbing the system. Clusters I and II represent groups of genes whose expression is affected by the expression of Aβ and is either repressed or rescued by the activation of Wnt signaling, and likely contain genes responsible for the observed differences in lifespan.

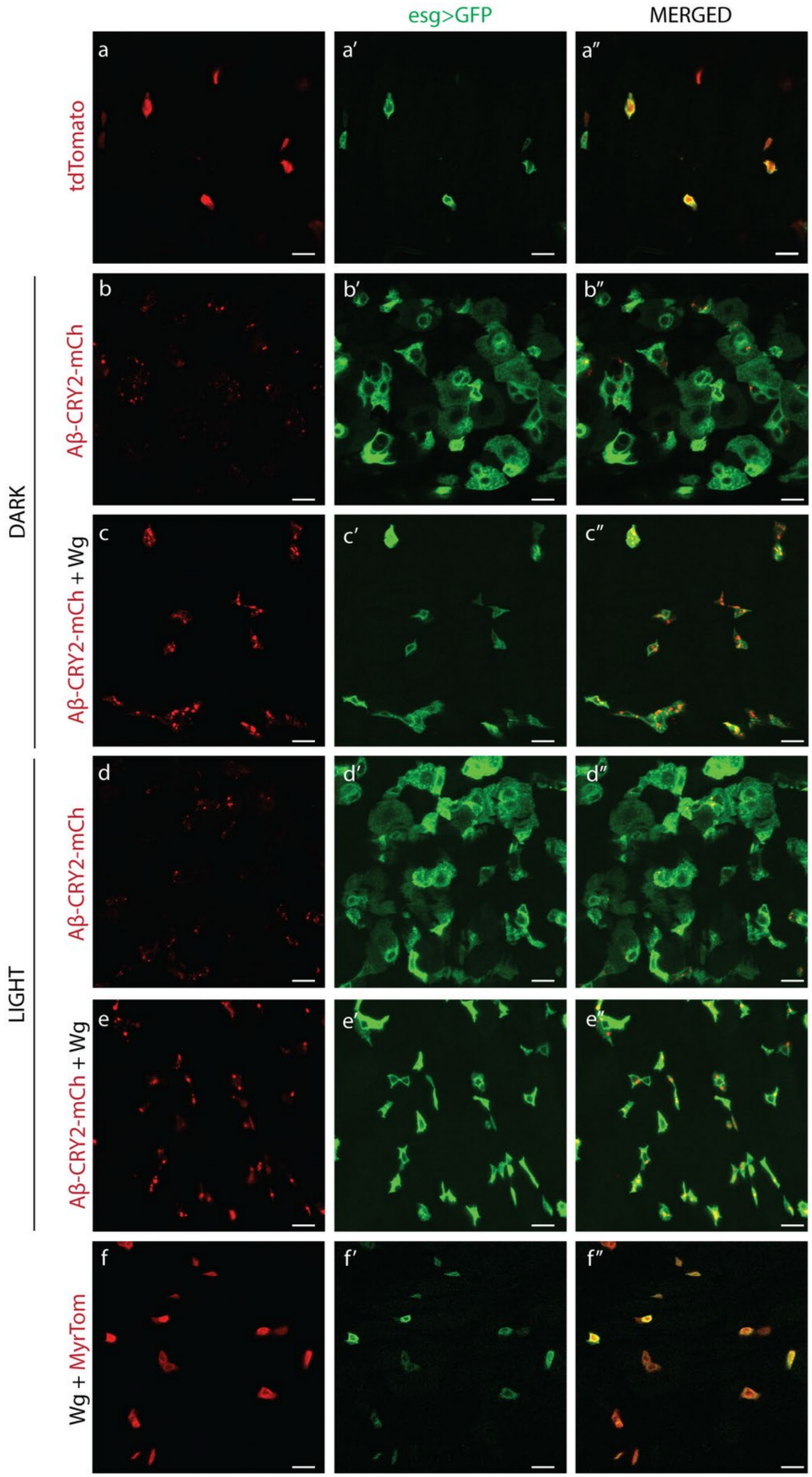

Figure 3. Wnt and amyloid expression in ISCs. Images of midgut sections of (**a**–**a″**) esg-Gal4 > UAS-GFP, UAS-Td-Tomato flies, (**b**–**b″**) esg-Gal4 > UAS-GFP, UAS-Aβ^{1-42}-CRY2-mCh flies kept in the dark, (**c**–**c″**) esgGal4 > UAS-GFP, UAS-wg, UAS-Aβ^{1-42}-CRY2-mCh flies kept in the dark, (**d**–**d″**) esg-Gal4 > UAS-GFP, UAS-Aβ^{1-42}-CRY2-mCh flies kept in the light, (**e**–**e″**) esg-Gal4 > UAS-GFP, UAS-wg, UAS-Aβ^{1-42}-CRY2-mCh flies kept in the light and (**f**–**f″**) esg-Gal4 > UAS-GFP, UAS-wg, UAS-myr-Tomato flies. Scale bar represents 10 μm.

(a)

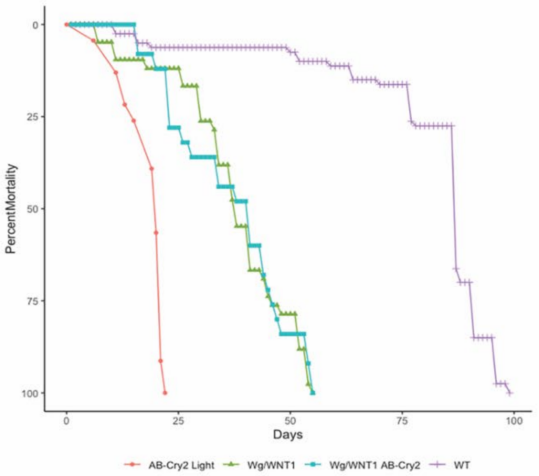

(b)

Sample	n	Mean no. of days	Corrected p-value (vs TdTomato)
TdTomato	80	80.66 ± 2.23	
Wg	42	37.36 ± 1.97	<0.01
Aβ-Cry2-mCh + Wg	25	36.76 ± 2.50	<0.01
Aβ-Cry2-mCh Light	23	18.17 ± 0.89	<0.01

(c)

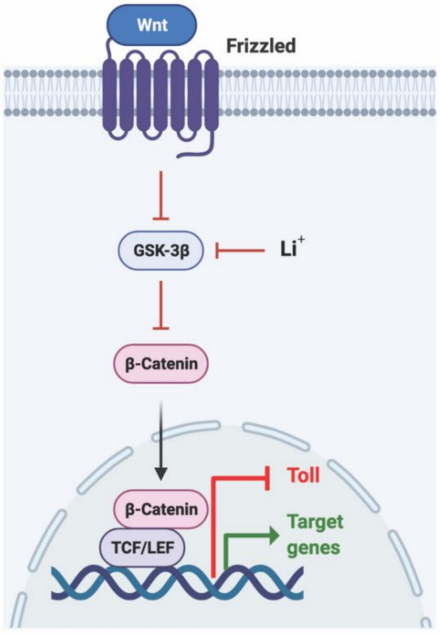

Figure 4. Lifespan decrease rescued by Wnt expression. Lifespan analysis of flies expressing TdTomato (control), Wg, Aβ-CRY2-mCh + Wg and Aβ-CRY2-mCh in gut stem cells. Genotype: *TdTomato*—esg-Gal4>UAS-GFP, UAS-Td-Tomato; *Wg*—esg-Gal4> UAS-GFP, UAS-wg, *Aβ-CRY2-mCh + Wg*—esg-Gal4> UAS-GFP, UAS-wg, UAS-Aβ^{1-42}-CRY2-mCh; *Aβ-CRY2-mCh*—esg-Gal4> UAS-GFP, UAS-Aβ^{1-42}-CRY2-mCh. (**a**) The lifespan curves for the various genotypes, and (**b**) table showing the number of subjects with mean lifespans and *p*-values. (**c**) Diagram showing lithium-induced activation of the Wnt pathway inhibiting Toll signalling. Raw data provided in Supplemental Table S4.

Within Cluster I, we identified several potential targets (Figure 5f), including CG5214, a succinyltransferase that regulates post-translational modifications of proteins and is associated with aging [66,67], and the transcriptional coactivator spargel (*srl*), the *Drosophila* homolog of *PGC-1αβ*–a gene involved in mitochondrial homeostasis and Insulin-TOR signaling, which has been implicated in AD pathogenesis [68,69]. We further observed genes related to innate immune activation, such as Persephone (*psh*), a serine protease that

is involved in regulating Toll pathway activation [70]. Overall, our transcriptomic analysis showed Wnt rescuing the expression of components of key neuroprotective pathways, while acting against most of the known processes involved in AD pathogenesis.

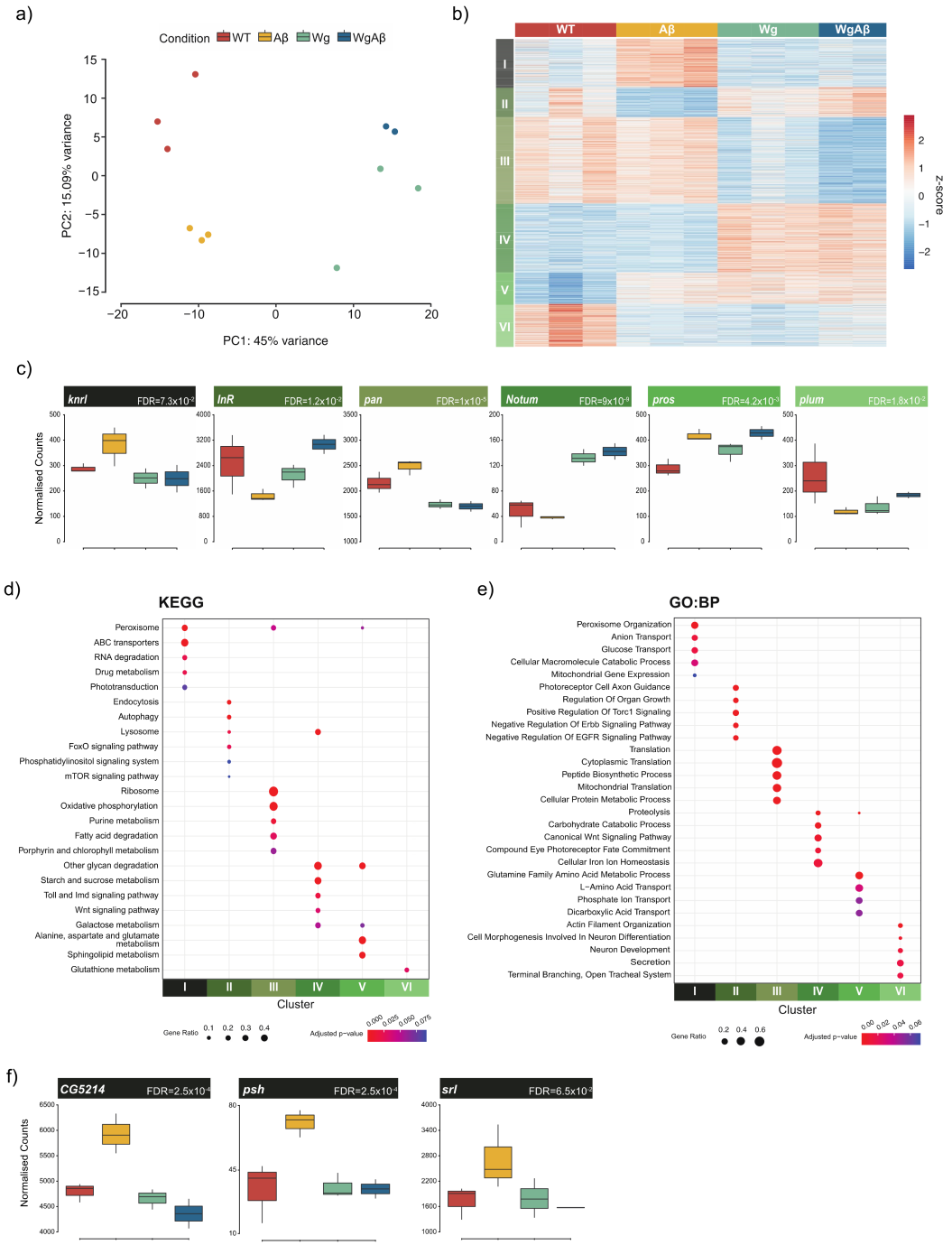

Figure 5. Gene expression changes in response to amyloid and Wnt. (**a**) Principal components analysis of RNA-seq data reveals clear separation of samples by experimental condition (**b**) Clustering of differentially expressed genes identifies six clusters with distinct expression patterns across the four conditions (**c**) Expression profiles of representative genes for each of the six clusters (**d**) KEGG pathway enrichments identifies key developmental and homeostatic pathways associated with the individual clusters (FDR < 10%) (**e**) Biological process (GO:BP) analysis identifies distinct processes enriched in each of the clusters (FDR < 10%). (**f**) Expression profiles of genes from Cluster I which are relevant to AD biology.

In AD, inflammation plays an important role in disease progression [71]. The up-regulation of *psh* in Aβ is indicative of the activation of the Toll pathway, a key pathway involved in inflammation and innate immunity. We used the Toll receptor, a key activator of innate immune response, to assay the inflammatory activity as it relates to lifespan. We used an optogenetic version of Toll; we had previously constructed and tested its effect on fly lifespans [46]. We expressed Toll-Cry2-mCherry in adult flies using the esg-Gal4 system to target ISCs, and in the whole fly using Arm-Gal4. Whole animal expression of Toll-Cry2-mCherry along with light exposure led to rapid death (Figure 6). The expression only in ISCs was less damaging, but the activation of the Toll pathway by Toll-Cry2-mCherry led to a reduction in lifespan, comparable to the effect of $A\beta^{1-42}$-CRY2-mCh. The effects were comparable when tested in flies kept in the dark. Overall, modulating the level of innate immune response led to lifespan shortening.

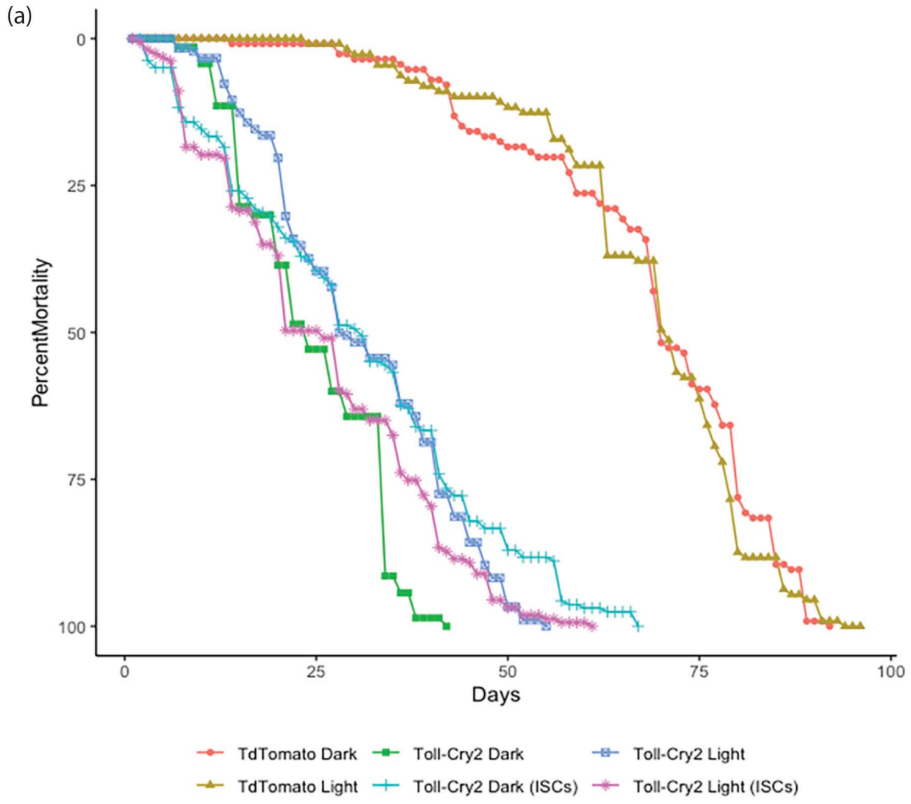

(b)

Sample	n	Mean no. of days	Corrected p-value (vs TdTomato Dark)
TdTomato Dark	114	68.50 ± 1.55	
TdTomato Light	111	68.52 ± 1.41	1
Toll-Cry2 Dark	70	24.66 ± 1.08	<0.001
Toll-Cry2 Light	182	31.12 ± 0.92	<0.001
Toll-Cry2 Dark (ISCs)	162	30.59 ± 0.92	<0.001
Toll-Cry2 Light (ISCs)	157	26.00 ± 1.13	<0.001

Figure 6. Activated Toll reduces lifespan. Lifespan analysis of TdTomato (control) dark and light, Toll-Cry2-mCh dark and light in the whole fly, Toll-Cry2-mCh dark and light expression in the ISCs only. Genotype: TdTomato—Arm-Gal4 > UAS-Td-Tomato; Toll-Cry2—ArmGal4 > UAS-Toll-Cry2-mCh; Toll-Cry2 (ISCs)—esg-Gal4 > UAS-GFP, UAS-Toll-Cry2-mCh. (**a**) The lifespan curves for the various genotypes, and (**b**) table showing the number of subjects with mean lifespans and *p*-values. Raw data provided in Supplemental Table S5.

Finally, we looked at the effect of *persephone* on *Drosophila* lifespan, as this gene was a major target identified by the RNA sequencing experiment (Figure 5f). Loss of *persephone* should lead to lower inflammation, since Toll activity would be reduced [70,72]. We observed an increase in median lifespan of *Drosophila* expressing RNAi to knockdown *psh* as compared to control flies (Figure 7). In addition, we looked at a stronger loss of immune response by knocking down the *Dorsal-related immunity factor* (*Dif*) [73]. Loss of *Dif* led to a reduction in lifespan, suggesting that a strong loss of immune response remains detrimental (Figure 7). Overall, we find that a reduction in inflammation is beneficial, whereas strong inflammation or strong loss of immune response remains detrimental.

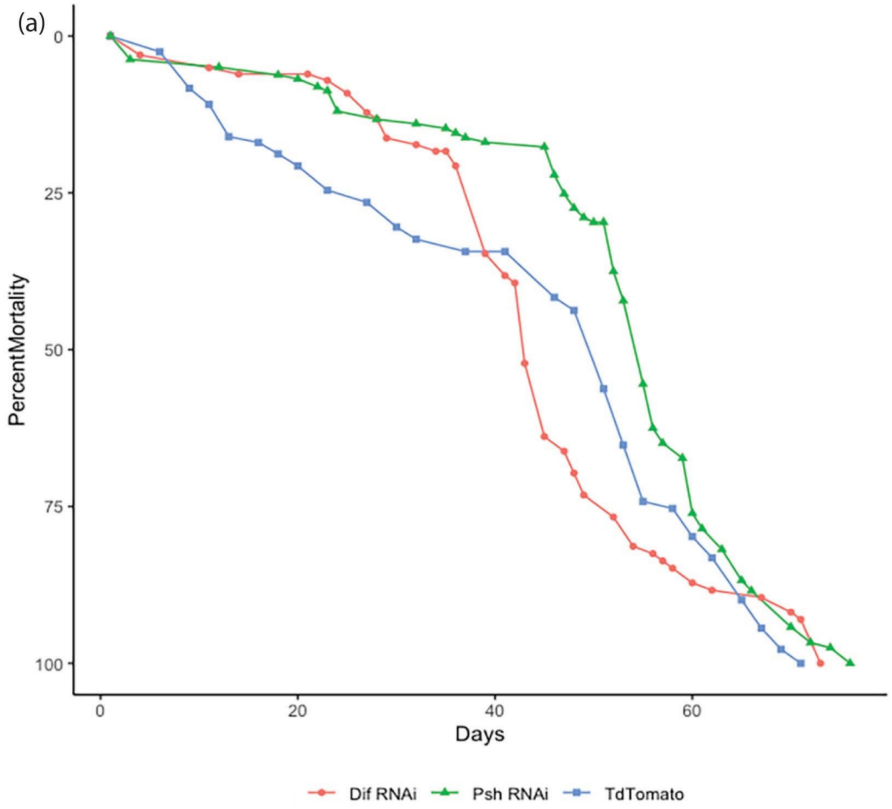

(b) Sample	n	Mean no. of Days	Corrected p-value (vs TdTomato)
TdTomato	120	43.59	
Dif RNAi	99	42.36	0.02
Psh RNAi	161	50.56	0.02

Figure 7. Knockdown of persephone extends lifespan. Lifespan analysis of TdTomato (control), psh-RNAi and Dif-RNAi in the whole fly. Genotype: TdTomato—Arm-Gal4 > UAS-Td-Tomato; Dif RNAi—ArmGal4 > UAS-Dif RNAi; Psh RNAi—Arm-Gal4 > UAS-Psh RNAi. (**a**) The lifespan curves for the various genotypes, and (**b**) table showing the number of subjects with mean lifespans and *p*-values. Raw data provided in Supplemental Table S6.

4. Discussion

In an update to our previously published study, we looked at the mechanism that lithium used to extend the lifespan of *Drosophila* expressing $A\beta^{1-42}$-CRY2-mCh. We postulated that the Wnt pathway was the key component to this based on previous studies [22,23,34,74]. However, we were unable to test the model in embryonic neurogenesis as the application of lithium and Wnt to embryos proved either technically or genetically problematic, and instead we investigated this in the *Drosophila* gut, an adult homeostasis

model. The overexpression of Wnt in ISCs was found to ameliorate the homeostatic and lethal consequences of $A\beta^{1-42}$-CRY2-mCh expression. We found several metabolic, proteostatic and inflammatory pathways to be activated by $A\beta^{1-42}$-CRY2-mCh and repressed by Wnt. We propose that Wnt's role in promoting homeostasis in stem cells can be extended to prevent some of the detrimental effects of $A\beta^{1-42}$-CRY2-mCh expression by preventing Toll pathway activation. We show that Toll activation is just as detrimental as $A\beta^{1-42}$-CRY2-mCh expression, while *psh* knockdown is beneficial, and propose that Wnt prevents Toll hyperactivation, leading to amelioration of amyloid-based detriments.

As we and others have previously proposed that lithium could be used as a treatment for AD [75,76], by narrowing the effect of lithium to Wnt activation, this creates the possibility of using Wnt activating drugs in AD treatment, especially as one has recently been shown to be life extending [77]. Most importantly, the homeostatic role of Wnt is not the only developmental signal that promotes homeostasis and prevents amyloid detriments. Recently, a role for Hedgehog was discovered in glial cells to promote lifespan and prevent amyloid-dependent neurodegeneration [78]. These findings together suggest that stem cell homeostasis and the re-activation of developmental pathways may be key mechanisms that could be targeted to prevent neurodegeneration.

Supplementary Materials: The following supporting information can be downloaded at: https://www.mdpi.com/article/10.3390/cells11020281/s1, Supplementary Figure S1: Expression profiles of genes contributing to enrichment of key processes/pathways identified as enriched in Cluster I.; Supplementary Figure S2: Expression profiles of genes contributing to enrichment of key processes/pathways identified as enriched in Cluster II. Supplemental Videos, Video S1. Elav-Gal4>UAS-Aβ1-42-CRY2-mCh, Repo-QF2>QUAS-GFP embryos kept in the dark and imaged for neurons using mCherry and glial cells using low (5%) blue laser power to allow imaging of glial cells without inducing pathological clustering. Scale bar represents 50 μm. Video S2. Elav-Gal4>UAS-Aβ1-42-CRY2-mCh, Repo-QF2>QUAS-GFP embryos kept in the light and imaged for neurons using mCherry and glial cells using high (10%) blue laser power to allow imaging of glial cells to induce clustering. Scale bar represents 50 μm. Video S3. Embryos expressing Td-Tomato in the nervous system (Elav-Gal4>UAS-Td-Tomato) develop normally. Scale bar represents 20 μm. Video S4. Expressing wg in the nervous system (Elav-Gal4>UAS-wg, UAS-RFP) is lethal to the embryos. Scale bar represents 20 μm. Supplemental Tables: Table S1: Results from differential expression analysis, Table S2: GO:BP enrichment analysis results for each cluster, Table S3: KEGG pathway enrichment analysis results for each cluster, Table S4: Raw date for Amyloid Lifespans, Table S5: Raw data for Toll Lifespans, Table S6: Raw data for Persephone and Dif Lifespans.

Author Contributions: Conceptualization, P.K., N.H. and N.S.T.; methodology, P.K., E.H.Z.C., W.K.L. and J.L.; software E.H.Z.C.; investigation, P.K., E.H.Z.C., W.K.L. and J.L.; resources, N.H. and N.S.T.; writing—original draft preparation, N.S.T.; writing—review and editing, P.K., E.H.Z.C., N.H. and N.S.T.; funding acquisition, N.S.T. and N.H. All authors have read and agreed to the published version of the manuscript.

Funding: We are thankful for the funding provided by AcRF grants IG19-SI102 and IG20-BG101to NST. NH and EHZC are supported by a Yale-NUS and Duke-NUS startup grant.

Institutional Review Board Statement: Not applicable.

Informed Consent Statement: Not applicable.

Data Availability Statement: RNA-seq data generated from this study have been deposited to NCBI GEO (GSE181844) https://www.ncbi.nlm.nih.gov/geo/query/acc.cgi?acc=GSE181844 (accessed on 10 August 2021). All code necessary to recreate the results from the RNA-seq analysis is available from: https://github.com/harmstonlab/Ab (accessed on 5 August 2021).

Conflicts of Interest: The authors declare no conflict of interest.

References

1. De-Paula, V.J.; Radanovic, M.; Diniz, B.S.; Forlenza, O.V. Alzheimer's disease. *Sub-Cell. Biochem.* **2012**, *65*, 329–352.
2. Kumar, A.; Singh, A.; Ekavali. A review on alzheimer's disease pathophysiology and its management: An update. *Pharmacol. Rep. PR* **2015**, *67*, 195–203. [CrossRef] [PubMed]
3. Anderson, R.M.; Hadjichrysanthou, C.; Evans, S.; Wong, M.M. Why do so many clinical trials of therapies for alzheimer's disease fail? *Lancet* **2017**, *390*, 2327–2329. [CrossRef]
4. Lalli, G.; Schott, J.M.; Hardy, J.; De Strooper, B. Aducanumab: A new phase in therapeutic development for alzheimer's disease? *EMBO Mol. Med.* **2021**, *13*, e14781. [CrossRef] [PubMed]
5. Sevigny, J.; Chiao, P.; Bussiere, T.; Weinreb, P.H.; Williams, L.; Maier, M.; Dunstan, R.; Salloway, S.; Chen, T.; Ling, Y.; et al. The antibody aducanumab reduces abeta plaques in alzheimer's disease. *Nature* **2016**, *537*, 50–56. [CrossRef] [PubMed]
6. Cummings, J. Lessons learned from alzheimer disease: Clinical trials with negative outcomes. *Clin. Transl. Sci.* **2018**, *11*, 147–152. [CrossRef] [PubMed]
7. Cummings, J.; Lee, G.; Ritter, A.; Zhong, K. Alzheimer's disease drug development pipeline: 2018. *Alzheimer's Dement.* **2018**, *4*, 195–214. [CrossRef]
8. Hardy, J.A.; Higgins, G.A. Alzheimer's disease: The amyloid cascade hypothesis. *Science* **1992**, *256*, 184–185. [CrossRef]
9. Driscoll, I.; Troncoso, J. Asymptomatic alzheimer's disease: A prodrome or a state of resilience? *Curr. Alzheimer Res.* **2011**, *8*, 330–335. [CrossRef]
10. Ferreira, S.T.; Klein, W.L. The abeta oligomer hypothesis for synapse failure and memory loss in alzheimer's disease. *Neurobiol. Learn. Mem.* **2011**, *96*, 529–543. [CrossRef]
11. Lim, C.H.; Kaur, P.; Teo, E.; Lam, V.Y.M.; Zhu, F.; Kibat, C.; Gruber, J.; Mathuru, A.S.; Tolwinski, N.S. Application of optogenetic amyloid-beta distinguishes between metabolic and physical damages in neurodegeneration. *eLife* **2020**, *9*, e52589. [CrossRef]
12. Lim, W.K.; Kaur, P.; Huang, H.; Jo, R.S.; Ramamoorthy, A.; Ng, L.F.; Suresh, J.; Maisha, F.I.; Mathuru, A.S.; Tolwinski, N.S. Optogenetic approaches for understanding homeostatic and degenerative processes in drosophila. *Cell. Mol. Life Sci.* **2021**, *78*, 5865–5880. [CrossRef] [PubMed]
13. Möglich, A.; Moffat, K. Engineered photoreceptors as novel optogenetic tools. *Photochem. Photobiol. Sci.* **2010**, *9*, 1286–1300. [CrossRef] [PubMed]
14. Fenno, L.; Yizhar, O.; Deisseroth, K. The development and application of optogenetics. *Annu. Rev. Neurosci.* **2011**, *34*, 389–412. [CrossRef] [PubMed]
15. Mas, P.; Devlin, P.F.; Panda, S.; Kay, S.A. Functional interaction of phytochrome b and cryptochrome 2. *Nature* **2000**, *408*, 207–211. [CrossRef]
16. Clevers, H. Wnt/beta-catenin signaling in development and disease. *Cell* **2006**, *127*, 469–480. [CrossRef]
17. Wodarz, A.; Nusse, R. Mechanisms of wnt signaling in development. *Annu. Rev. Cell. Dev. Biol.* **1998**, *14*, 59–88. [CrossRef]
18. Hu, D.J.; Yun, J.; Elstrott, J.; Jasper, H. Non-canonical wnt signaling promotes directed migration of intestinal stem cells to sites of injury. *Nat. Commun.* **2021**, *12*, 7150. [CrossRef]
19. Dunn, N.R.; Tolwinski, N.S. Ptk7 and mcc, unfancied components in non-canonical wnt signaling and cancer. *Cancers* **2016**, *8*, 68. [CrossRef]
20. Tian, A.; Benchabane, H.; Wang, Z.; Ahmed, Y. Regulation of stem cell proliferation and cell fate specification by wingless/wnt signaling gradients enriched at adult intestinal compartment boundaries. *PLoS Genet.* **2016**, *12*, e1005822. [CrossRef]
21. Tian, A.; Duwadi, D.; Benchabane, H.; Ahmed, Y. Essential long-range action of wingless/wnt in adult intestinal compartmentalization. *PLoS Genet.* **2019**, *15*, e1008111. [CrossRef] [PubMed]
22. Ng, L.F.; Kaur, P.; Bunnag, N.; Suresh, J.; Sung, I.C.H.; Tan, Q.H.; Gruber, J.; Tolwinski, N.S. Wnt signaling in disease. *Cells* **2019**, *8*, 826. [CrossRef] [PubMed]
23. Suresh, J.; Khor, I.W.; Kaur, P.; Heng, H.L.; Torta, F.; Dawe, G.S.; Tai, E.S.; Tolwinski, N.S. Shared signaling pathways in alzheimer's and metabolic disease may point to new treatment approaches. *FEBS J.* **2021**, *288*, 3855–3873. [CrossRef]
24. Ali, A.; Ali, A.; Ahmad, W.; Ahmad, N.; Khan, S.; Nuruddin, S.M.; Husain, I. Deciphering the role of wnt signaling in metabolic syndrome–linked alzheimer's disease. *Mol. Neurobiol.* **2020**, *57*, 302–314. [CrossRef] [PubMed]
25. Nusse, R.; Clevers, H. Wnt/beta-catenin signaling, disease, and emerging therapeutic modalities. *Cell* **2017**, *169*, 985–999. [CrossRef]
26. Clevers, H.; Nusse, R. Wnt/beta-catenin signaling and disease. *Cell* **2012**, *149*, 1192–1205. [CrossRef] [PubMed]
27. Cadigan, K.M.; Nusse, R. Wnt signaling: A common theme in animal development. *Genes Dev.* **1997**, *11*, 3286–3305. [CrossRef] [PubMed]
28. Schlessinger, K.; Hall, A.; Tolwinski, N. Wnt signaling pathways meet rho gtpases. *Genes Dev.* **2009**, *23*, 265–277. [CrossRef] [PubMed]
29. Tolwinski, N.S.; Wieschaus, E. A nuclear escort for beta-catenin. *Nat. Cell. Biol.* **2004**, *6*, 579–580. [CrossRef] [PubMed]
30. Kaplan, N.A.; Colosimo, P.F.; Liu, X.; Tolwinski, N.S. Complex interactions between gsk3 and apkc in drosophila embryonic epithelial morphogenesis. *PLoS One* **2011**, *6*, e18616. [CrossRef] [PubMed]
31. Martinez, M.; Inestrosa, N.C. The transcriptional landscape of alzheimer's disease and its association with wnt signaling pathway. *Neurosci. Biobehav. Rev.* **2021**, *128*, 454–466. [CrossRef]

32. Inestrosa, N.C.; Varela-Nallar, L. Wnt signaling in the nervous system and in alzheimer's disease. *J. Mol. Cell Biol* **2014**, *6*, 64–74. [CrossRef]
33. Yang, Y.; Zhang, Z. Microglia and wnt pathways: Prospects for inflammation in alzheimer's disease. *Front. Aging Neurosci.* **2020**, *12*, 110. [CrossRef]
34. Jia, L.; Piña-Crespo, J.; Li, Y. Restoring wnt/β-catenin signaling is a promising therapeutic strategy for alzheimer's disease. *Mol. Brain* **2019**, *12*, 1–11. [CrossRef]
35. Teo, E.; Ravi, S.; Barardo, D.; Kim, H.S.; Fong, S.; Cazenave-Gassiot, A.; Tan, T.Y.; Ching, J.; Kovalik, J.P.; Wenk, M.R.; et al. Metabolic stress is a primary pathogenic event in transgenic caenorhabditis elegans expressing pan-neuronal human amyloid beta. *eLife* **2019**, *8*, e50069. [CrossRef] [PubMed]
36. Kaur, P.; Saunders, T.E.; Tolwinski, N.S. Coupling optogenetics and light-sheet microscopy, a method to study wnt signaling during embryogenesis. *Sci. Rep.* **2017**, *7*, 16636. [CrossRef] [PubMed]
37. Brand, A.H.; Perrimon, N. Targeted gene expression as a means of altering cell fates and generating dominant phenotypes. *Development* **1993**, *118*, 401–415. [CrossRef]
38. McGuire, S.E.; Le, P.T.; Osborn, A.J.; Matsumoto, K.; Davis, R.L. Spatiotemporal rescue of memory dysfunction in drosophila. *Science* **2003**, *302*, 1765–1768. [CrossRef]
39. Lin, D.M.; Goodman, C.S. Ectopic and increased expression of fasciclin ii alters motoneuron growth cone guidance. *Neuron* **1994**, *13*, 507–523. [CrossRef]
40. Potter, C.J.; Tasic, B.; Russler, E.V.; Liang, L.; Luo, L. The q system: A repressible binary system for transgene expression, lineage tracing, and mosaic analysis. *Cell* **2010**, *141*, 536–548. [CrossRef]
41. Shearin, H.K.; Macdonald, I.S.; Spector, L.P.; Stowers, R.S. Hexameric gfp and mcherry reporters for the drosophila gal4, q, and lexa transcription systems. *Genetics* **2014**, *196*, 951–960. [CrossRef] [PubMed]
42. Pfeiffer, B.D.; Ngo, T.T.; Hibbard, K.L.; Murphy, C.; Jenett, A.; Truman, J.W.; Rubin, G.M. Refinement of tools for targeted gene expression in drosophila. *Genetics* **2010**, *186*, 735–755. [CrossRef]
43. Hays, R.; Gibori, G.B.; Bejsovec, A. Wingless signaling generates pattern through two distinct mechanisms. *Development* **1997**, *124*, 3727–3736. [CrossRef] [PubMed]
44. Bosch, J.A.; Colbeth, R.; Zirin, J.; Perrimon, N. Gene knock-ins in drosophila using homology-independent insertion of universal donor plasmids. *Genetics* **2020**, *214*, 75–89. [CrossRef]
45. Micchelli, C.A.; Perrimon, N. Evidence that stem cells reside in the adult drosophila midgut epithelium. *Nature* **2006**, *439*, 475–479. [CrossRef]
46. Bunnag, N.; Tan, Q.H.; Kaur, P.; Ramamoorthy, A.; Sung, I.C.H.; Lusk, J.; Tolwinski, N.S. An optogenetic method to study signal transduction in intestinal stem cell homeostasis. *J. Mol. Biol* **2020**, *432*, 3159–3176. [CrossRef]
47. White, P.; Vincent, J.-P. Uncoupling cadherin-based adhesion from wingless signalling in drosophila. *Nature* **1996**, *383*, 627–630.
48. Perkins, L.A.; Holderbaum, L.; Tao, R.; Hu, Y.; Sopko, R.; McCall, K.; Yang-Zhou, D.; Flockhart, I.; Binari, R.; Shim, H.-S. The transgenic rnai project at harvard medical school: Resources and validation. *Genetics* **2015**, *201*, 843–852. [CrossRef]
49. Kaur, P.; Lam, V.Y.M.; Mannava, A.G.; Suresh, J.; Jenny, A.; Tolwinski, N.S. Membrane targeting of disheveled can bypass the need for arrow/lrp5. *Sci. Rep.* **2017**, *7*, 6934. [CrossRef]
50. Kaur, P.; Jin, H.J.; Lusk, J.B.; Tolwinski, N.S. Modeling the role of wnt signaling in human and drosophila stem cells. *Genes* **2018**, *9*, 201. [CrossRef]
51. Kaur, P.; Kibat, C.; Teo, E.; Gruber, J.; Mathuru, A.; Tolwinski, N.S. Use of optogenetic amyloid-β to monitor protein aggregation in drosophila melanogaster, danio rerio and caenorhabditis elegans. *Bio-Protocol* **2020**, *10*, e3856. [CrossRef]
52. Schneider, C.A.; Rasband, W.S.; Eliceiri, K.W. Nih image to imagej: 25 years of image analysis. *Nat. Methods* **2012**, *9*, 671–675. [CrossRef] [PubMed]
53. Dobin, A.; Davis, C.A.; Schlesinger, F.; Drenkow, J.; Zaleski, C.; Jha, S.; Batut, P.; Chaisson, M.; Gingeras, T.R. Star: Ultrafast universal rna-seq aligner. *Bioinformatics* **2013**, *29*, 15–21. [CrossRef] [PubMed]
54. Li, B.; Dewey, C.N. Rsem: Accurate transcript quantification from rna-seq data with or without a reference genome. *BMC Bioinform.* **2011**, *12*, 1–16. [CrossRef] [PubMed]
55. Love, M.I.; Huber, W.; Anders, S. Moderated estimation of fold change and dispersion for rna-seq data with deseq2. *Genome Biol.* **2014**, *15*, 550. [CrossRef]
56. Chen, E.Y.; Tan, C.M.; Kou, Y.; Duan, Q.; Wang, Z.; Meirelles, G.V.; Clark, N.R.; Ma'ayan, A. Enrichr: Interactive and collaborative html5 gene list enrichment analysis tool. *BMC Bioinform.* **2013**, *14*, 128. [CrossRef] [PubMed]
57. Kuleshov, M.V.; Jones, M.R.; Rouillard, A.D.; Fernandez, N.F.; Duan, Q.; Wang, Z.; Koplev, S.; Jenkins, S.L.; Jagodnik, K.M.; Lachmann, A.; et al. Enrichr: A comprehensive gene set enrichment analysis web server 2016 update. *Nucleic Acids Res.* **2016**, *44*, W90–W97. [CrossRef]
58. Xie, Z.; Bailey, A.; Kuleshov, M.V.; Clarke, D.J.B.; Evangelista, J.E.; Jenkins, S.L.; Lachmann, A.; Wojciechowicz, M.L.; Kropiwnicki, E.; Jagodnik, K.M.; et al. Gene set knowledge discovery with enrichr. *Curr. Protoc.* **2021**, *1*, e90. [CrossRef]
59. Han, S.K.; Lee, D.; Lee, H.; Kim, D.; Son, H.G.; Yang, J.S.; Lee, S.V.; Kim, S. Oasis 2: Online application for survival analysis 2 with features for the analysis of maximal lifespan and healthspan in aging research. *Oncotarget* **2016**, *7*, 56147–56152. [CrossRef]
60. Jasper, H. Intestinal stem cell aging: Origins and interventions. *Annu. Rev. Physiol.* **2020**, *82*, 203–226. [CrossRef]
61. Zhang, P.; Edgar, B.A. Insect gut regeneration. *Cold Spring Harb. Perspect. Biol.* **2021**, a040915. [CrossRef] [PubMed]

62. Kou, J.; Kovacs, G.G.; Hoftberger, R.; Kulik, W.; Brodde, A.; Forss-Petter, S.; Honigschnabl, S.; Gleiss, A.; Brugger, B.; Wanders, R.; et al. Peroxisomal alterations in alzheimer's disease. *Acta Neuropathol.* **2011**, *122*, 271–283. [CrossRef]
63. Jo, D.S.; Park, N.Y.; Cho, D.H. Peroxisome quality control and dysregulated lipid metabolism in neurodegenerative diseases. *Exp. Mol. Med.* **2020**, *52*, 1486–1495. [CrossRef]
64. Oddo, S. The role of mtor signaling in alzheimer disease. *Front. Biosci.* **2012**, *4*, 941–952. [CrossRef]
65. Cai, Z.; Chen, G.; He, W.; Xiao, M.; Yan, L.J. Activation of mtor: A culprit of alzheimer's disease? *Neuropsychiatr. Dis. Treat.* **2015**, *11*, 1015–1030. [CrossRef] [PubMed]
66. Hong, S.Y.; Ng, L.T.; Ng, L.F.; Inoue, T.; Tolwinski, N.S.; Hagen, T.; Gruber, J. The role of mitochondrial non-enzymatic protein acylation in ageing. *PLoS ONE* **2016**, *11*, e0168752. [CrossRef] [PubMed]
67. Bonnay, F.; Veloso, A.; Steinmann, V.; Kocher, T.; Abdusselamoglu, M.D.; Bajaj, S.; Rivelles, E.; Landskron, L.; Esterbauer, H.; Zinzen, R.P.; et al. Oxidative metabolism drives immortalization of neural stem cells during tumorigenesis. *Cell* **2020**, *182*, 1490–1507.e1419. [CrossRef]
68. Tiefenbock, S.K.; Baltzer, C.; Egli, N.A.; Frei, C. The drosophila pgc-1 homologue spargel coordinates mitochondrial activity to insulin signalling. *EMBO J.* **2010**, *29*, 171–183. [CrossRef]
69. Mukherjee, S.; Duttaroy, A. Spargel/dpgc-1 is a new downstream effector in the insulin-tor signaling pathway in drosophila. *Genetics* **2013**, *195*, 433–441. [CrossRef]
70. Ligoxygakis, P.; Pelte, N.; Hoffmann, J.A.; Reichhart, J.M. Activation of drosophila toll during fungal infection by a blood serine protease. *Science* **2002**, *297*, 114–116. [CrossRef] [PubMed]
71. Kinney, J.W.; Bemiller, S.M.; Murtishaw, A.S.; Leisgang, A.M.; Salazar, A.M.; Lamb, B.T. Inflammation as a central mechanism in alzheimer's disease. *Alzheimer's Dement. Transl. Res. Clin. Interv.* **2018**, *4*, 575–590. [CrossRef] [PubMed]
72. Issa, N.; Guillaumot, N.; Lauret, E.; Matt, N.; Schaeffer-Reiss, C.; Van Dorsselaer, A.; Reichhart, J.-M.; Veillard, F. The circulating protease persephone is an immune sensor for microbial proteolytic activities upstream of the drosophila toll pathway. *Mol. Cell* **2018**, *69*, 539–550.e536. [CrossRef]
73. Ip, Y.T.; Reach, M.; Engstrom, Y.; Kadalayil, L.; Cai, H.; González-Crespo, S.; Tatei, K.; Levine, M. Dif, a dorsal-related gene that mediates an immune response in drosophila. *Cell* **1993**, *75*, 753–763. [CrossRef]
74. Palomer, E.; Buechler, J.; Salinas, P.C. Wnt signaling deregulation in the aging and alzheimer's brain. *Front. Cell. Neurosci.* **2019**, *13*, 227. [CrossRef]
75. Sofola-Adesakin, O.; Castillo-Quan, J.I.; Rallis, C.; Tain, L.S.; Bjedov, I.; Rogers, I.; Li, L.; Martinez, P.; Khericha, M.; Cabecinha, M.; et al. Lithium suppresses abeta pathology by inhibiting translation in an adult drosophila model of alzheimer's disease. *Front. Aging Neurosci.* **2014**, *6*, 190. [CrossRef]
76. Teo, E.; Fong, S.; Tolwinski, N.; Gruber, J. Drug synergy as a strategy for compression of morbidity in a caenorhabditis elegans model of alzheimer's disease. *Geroscience* **2020**, *42*, 849–856. [CrossRef]
77. Castillo-Quan, J.I.; Tain, L.S.; Kinghorn, K.J.; Li, L.; Gronke, S.; Hinze, Y.; Blackwell, T.K.; Bjedov, I.; Partridge, L. A triple drug combination targeting components of the nutrient-sensing network maximizes longevity. *Proc. Natl. Acad. Sci. USA* **2019**, *116*, 20817–20819. [CrossRef] [PubMed]
78. Rallis, A.; Navarro, J.A.; Rass, M.; Hu, A.; Birman, S.; Schneuwly, S.; Therond, P.P. Hedgehog signaling modulates glial proteostasis and lifespan. *Cell Rep.* **2020**, *30*, 2627–2643.e5. [CrossRef]